

Provided for non-commercial research and education use.  
Not for reproduction, distribution or commercial use.



This article appeared in a journal published by Elsevier. The attached copy is furnished to the author for internal non-commercial research and education use, including for instruction at the authors institution and sharing with colleagues.

Other uses, including reproduction and distribution, or selling or licensing copies, or posting to personal, institutional or third party websites are prohibited.

In most cases authors are permitted to post their version of the article (e.g. in Word or Tex form) to their personal website or institutional repository. Authors requiring further information regarding Elsevier's archiving and manuscript policies are encouraged to visit:

<http://www.elsevier.com/copyright>

ELSEVIER  
MASSON

Disponible en ligne sur  
**SciVerse ScienceDirect**  
 www.sciencedirect.com

Elsevier Masson France  
**EM|consulte**  
 www.em-consulte.com

---



---

**IRBM**


---



---

IRBM 34 (2013) 33–37

Digital technologies for healthcare

# Multiscale optical flow computation from the monogenic signal

M. Alessandrini<sup>a,\*</sup>, O. Bernard<sup>a</sup>, A. Basarab<sup>b</sup>, H. Liebgott<sup>a</sup>

<sup>a</sup> Université de Lyon, CREATIS, CNRS UMR5220, Inserm U1044, INSA-Lyon, Université Lyon 1, Lyon, France

<sup>b</sup> Université de Toulouse; IRIT, CNRS UMR5505, 118, route de Narbonne, 31062 Toulouse cedex 9, France

Received 9 November 2012; received in revised form 18 December 2012; accepted 19 December 2012

Available online 12 February 2013

---

## Abstract

We have developed an algorithm for the estimation of cardiac motion from medical images. The algorithm exploits monogenic signal theory, recently introduced as an N-dimensional generalization of the analytic signal. The displacement is computed locally by assuming the conservation of the monogenic phase over time. A local affine displacement model replaces the standard translation model to account for more complex motions as contraction/expansion and shear. A coarse-to-fine B-spline scheme allows a robust and effective computation of the models parameters and a pyramidal refinement scheme helps handle large motions. Robustness against noise is increased by replacing the standard pointwise computation of the monogenic orientation with a more robust least-squares orientation estimate. This paper reviews the results obtained on simulated cardiac images from different modalities, namely 2D and 3D cardiac ultrasound and tagged magnetic resonance. We also show how the proposed algorithm represents a valuable alternative to state-of-the-art algorithms in the respective fields.

© 2013 Elsevier Masson SAS. All rights reserved.

---

## 1. Introduction

The monogenic signal has been recently introduced by Felsberg and Sommer [1] as an extension of the analytic signal concept to multiple dimensions. Similarly to the latter, the monogenic signal provides the local amplitude and local phase signal features. It also contains information on the local orientation. These three local features are pointwise orthogonal, which means that they represent independent information: the local amplitude represents the local intensity or dynamics, the local phase describes the local symmetry or grey value transition, and the local orientation describes the direction of the highest signal variance.

Decoupling the local energy from the image structure, accounted for by phase and orientation, has made it possible to derive effective solutions to a number of image-processing problems, in particular when the more traditional pixel intensity cannot be considered as a reliable feature. In this context, we have recently proposed an original optical flow algorithm for the analysis of heart motion based on the monogenic phase [2].

Temporal brightness variations are indeed the norm in many medical imaging modalities such as ultrasound and MRI, and this fact negatively affects the performance of intensity based algorithms [2].

Thanks to its general formulation, the proposed algorithm is suitable for images from several imaging modalities. In particular, we summarize in this paper some of the results we have obtained on 2D and 3D cardiac ultrasound and on tagged MRI. In all cases, the proposed algorithm was shown to be competitive with state-of-the-art algorithms in the respective fields and extremely effective from a computational point of view.

The paper proceeds as follows. In Section 2.1, the monogenic signal theory is briefly resumed. In Section 2.2, the optical flow estimation algorithm presented in [2] is described. In Section 3, the results are presented. Concluding remarks are left to Section 4.

## 2. Proposed optical flow estimation algorithm

### 2.1. Monogenic signal computation

Only the most basic aspects of the monogenic signal computation are given here, the reader is otherwise addressed to [3] and the references therein for a theoretically founded derivation.

---

\* Corresponding author. CREATIS, INSA-Lyon, bâtiment Blaise-Pascal, 7, avenue Jean-Capelle, 69621 Villeurbanne cedex, France.

E-mail address: [martino.alessandrini@creatis.insa-lyon.fr](mailto:martino.alessandrini@creatis.insa-lyon.fr) (M. Alessandrini).

The monogenic signal provides the features local phase  $\phi(x)$ , orientation  $\theta(x)$  and amplitude  $A(x)$  of an image  $I(x)$ , where  $x = [x, y]^T$  is the pixel position. These quantities are computed pointwise from the responses to three 2D spherical quadrature filters (SQF) obtained as follows: one even rotation invariant bandpass filter and two *odd* filters, computed from the Riesz transform of the even one. Among the existing SQF families, we adopt in this work difference of Poisson (DoP) [3].

Alternatively to the standard pointwise estimate we employ a more robust least-squares technique for the computation of  $\theta$  [4]. This is obtained by maximizing the directional Hilbert transform  $H_\theta I(x)$  averaged over a local neighborhood, here a Gaussian kernel with variance  $\sigma^2$ , denoted by  $\nu_\sigma$ :

$$\theta(x) = \arg \max_{\theta' \in [-\pi, \pi]} \int_{\mathbb{R}^2} \nu_\sigma(x' - x) \cdot |H_{\theta'} I(x')|^2 dx'. \quad (1)$$

As shown in [4], the optimization problem is solved by the eigenvector associated to the maximum eigenvalue of the Riesz-transform counterpart of the image structure tensor.

## 2.2. Optical flow computation

Following [3], we compute the displacement  $d = [d_1, d_2]^T$  between two frames assuming the conservation of the monogenic phase over time  $\phi(x, t + 1) = \phi(x - d(x), t)$ . Then, assuming all points translate of the same quantity  $d_0$  within a local window  $w$  centered in  $x_0$ , the following linear system of equations is obtained:

$$\langle J \rangle_w d_0 = -\langle r_t \rangle_w, \quad J = f n n^T \quad (2)$$

where  $\langle v \rangle_w = \int w(x - x_0) v(x) dx$ ,  $r_t$  is the time derivative of the phase vector  $r = \phi \cdot n$ ,  $n = [\cos(\phi), \sin(\phi)]^T$  and  $f$  is the monogenic frequency, computed as  $f = (\nabla \phi)^T n$ , with  $\nabla = [\partial_x, \partial_y]^T$ . The expressions for the computation of  $r_t$  and  $f$  from SQF filter outputs can be found in [3].

Instead of the simple translation model, we adopt a more general affine model for the local displacement. In addition to translation, this accounts for rotation, expansion, compression and shear. Considering a window centered at the origin, the affine model is expressed as:

$$d(x) = A(x) u, \quad A = \begin{bmatrix} 1 & 0 & x & y & 0 & 0 \\ 0 & 1 & 0 & 0 & x & y \end{bmatrix} \quad (3)$$

where  $u = [d_{10}, d_{20}, d_{1x}, d_{1y}, d_{2x}, d_{2y}]^T$  is the new unknown vector:  $d_{10}$  and  $d_{20}$  correspond to the translation of the window center and  $d_{ik} = \partial_k d_i$ . Plugging (3) into (2) leads to an under-determined system of equations, whose least-squares solution is  $b = Mu$ , with  $b = -\langle A^T J^T r_t \rangle_w$  and  $M = \langle A^T J^T J A \rangle_w$ .

### 2.2.1. Multiscale choice of the window size

The choice of the window size is a tedious issue connected with local techniques: the assumed motion model (translational or affine) may not hold when the window is too big, otherwise, the adoption of an excessively small window may result in the well-known aperture problem. To circumvent this issue, in [5] Sühling et al. proposed a multiscale strategy for locally choosing

the most consistent window size. This is based on the possibility of computing the image moments, i.e., the entries of the system matrix  $M$  and the vector  $b$ , at multiple scales, by using an efficient B-spline coarse-to-fine strategy. In particular, they are obtained from window functions  $w$  that are progressively scaled and sub-sampled by a factor 2 in each dimension. Among the considered scales considered, the  $u^j$  producing the smallest residual error  $\|Mu^j - b\|_{\ell_2} / \|w\|_{\ell_1}$  is retained as the final displacement estimate. With this strategy, the scale providing the most consistent motion estimate is selected.

### 2.2.2. Iterative displacement refinement

The hypothesis of small displacements employed in differential techniques may be inadequate whenever the displacement is big or the image intensity profile is non-linear. To overcome this limitation we adopt an incremental coarse-to-fine refinement of the motion estimate: the coarsest scale provides a first estimate of the displacement, this estimate is then used to undo the motion and then the estimator is reapplied to the warped signals at the finer scale to find the residual motion.

## 3. Results

We evaluated the proposed algorithm on medical images from different modalities. In order to have a benchmark to compare to, we made use of synthetic sequences in all cases. Endpoint error:

$$EE = \|d - \bar{d}\|_{\ell_2} \quad (4)$$

was used for the evaluation, where  $d$  and  $\bar{d}$  denote estimated displacement and benchmark respectively. Unless explicitly mentioned, the displacement has to be intended as the one between two consecutive frames.

For display purposes, we adopted a color encoding of the velocities (Fig. 1), where the color indicates the direction of the displacement and the brightness expresses the magnitude.

Since what is of clinical interest is evaluating the mechanical properties of the cardiac muscle, in all cases we will measure the estimation error within the myocardium only (Fig. 2).

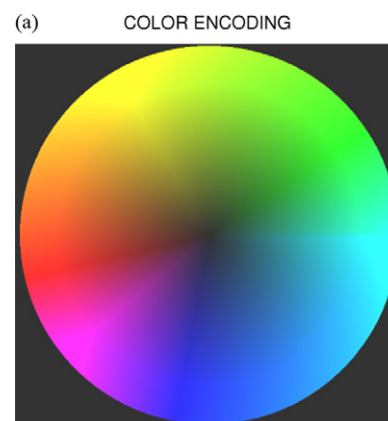


Fig. 1. Color encoding of velocities: x and y axes report the horizontal and vertical component of the velocity vector.

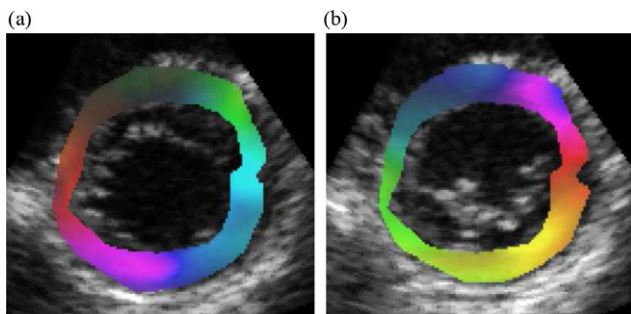


Fig. 2. Frames from a synthetic short-axis sequence during ventricular filling (diastole) (a) and ventricular ejection (systole) (b). The benchmark displacement field is superimposed. Note that the benchmark field reflects the physiological expansion and contraction during these two phases of the cardiac cycle.

### 3.1. 2D cardiac ultrasound

We evaluated our algorithm on custom made realistic synthetic cardiac ultrasound sequences, generated as described in [6]. Briefly, the simulated sequences are obtained by mimicking the aspect and the motion of a real echocardiographic acquisition taken as a template. For our evaluation, we considered simulated sequences from the two views the most commonly employed in the clinical practice, namely short-axis (SaX) and apical four chambers (A4C). Fig. 2 presents two frames from the simulated SaX sequence along with the benchmark motion.

We have compared our algorithm with the ones of Sühling et al. [5] and Felsberg [3]. Sühling’s algorithm exploits the standard intensity conservation assumption and, as in our case, employs an affine displacement model and a multiscale window selection. Differently, Felsberg’s algorithm makes use of the monogenic phase but employs a simple translation model and a window of fixed size.

Table 1 reports the average errors obtained on the entire simulated sequences (45 frames for the SaX view and 50 frames for the A4C). From Table 1 all the monogenic phase-based algorithms considered perform better than Sühling’s algorithm. This confirms that the monogenic phase is a more reliable feature than pixel intensity as far as medical ultrasound is concerned. Also, thanks to the affine model, the multiresolution window selection procedure and the pyramidal refinement, the proposed algorithm outperforms Felsberg’s one. For further results on 2D cardiac ultrasound we address the reader to [2,7].

### 3.2. 3D cardiac ultrasound

Despite our algorithm has been described in this paper for the displacement estimation from 2D images, an extension to

Table 1  
Endpoint error in pixels ( $\mu \pm \sigma$ ).

ALGORITHM	SEQUENCE	
	Apical 4 chambers	Short axis
Sühling	$0.395 \pm 0.338$	$0.396 \pm 0.346$
Felsberg	$0.315 \pm 0.257$	$0.364 \pm 0.293$
Proposed	$0.264 \pm 0.190$	$0.313 \pm 0.242$

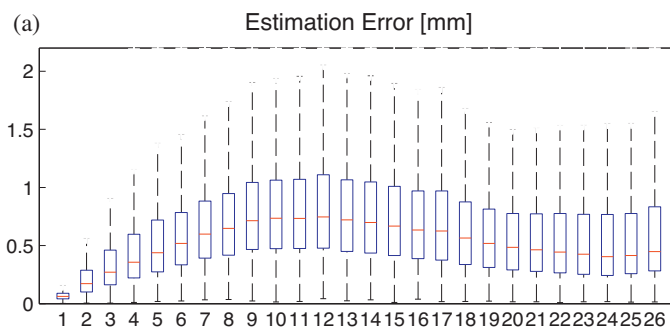


Fig. 3. Tracking error obtained with the proposed algorithm. Lower and upper limits of the box represent 25th and 75th percentile while the whiskers the 5th and 95th.

3D volumes can be almost straightforwardly derived [8]. Also in this case we evaluated our algorithm on synthetic 3D cardiac ultrasound data. In particular, the latter were provided as part of the “Tracking Challenge” promoted by the MICCAI conference [8].

The heart motion was simulated by displacing a set of point scatterers according to the electromechanical model of the myocardium proposed by Sermesant et al. [9]. From the time varying scatter map the ultrasound image formation was then simulated with the COLE software developed by Gao et al. [10]. Each simulated sequence realized a full cardiac cycle from one end-diastole to the next end-diastole. The algorithm evaluation was then performed by measuring the accuracy in tracking the scatterers employed in the simulation. Note that, differently from the previous cases, this implies computing the global displacement from the first frame of the sequence (end-diastole). The global field is therefore computed by accumulating the frame-by-frame displacements returned by the proposed algorithm.

In particular, we report here the result on one of the provided sequences representing a healthy heart. On Fig. 3 the error behavior over time is represented as a boxplot. As expected, the largest estimation error corresponds to the end-systolic instant, where the maximum displacement from the rest condition happens. Nevertheless, let us note that the average error remains much smaller with respect to the true maximum displacement that in the end-systolic instant reaches the value of 11.2 mm, also Fig. 4.

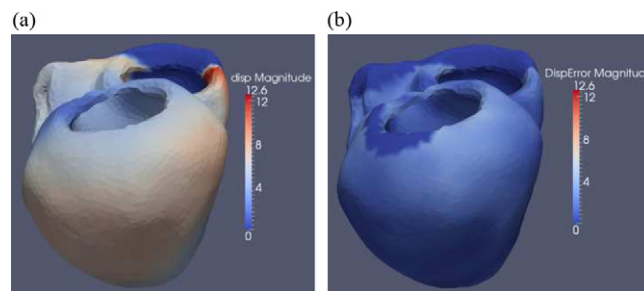


Fig. 4. Error maps at end-systole, when the displacement is the largest. (a) Real displacement of the scatterers with respect to the first frame of the sequence (end-diastole). This information provides the full-scale of the displacement to be estimated. (b) Estimation error obtained with the proposed algorithm. Note how it is considerably smaller than the maximum displacement reported in (a).

Table 2  
Endpoint error ( $\mu \pm \sigma$ ) in pixels on nine simulated sequences.

SEQUENCE	ALGORITHM	
	Proposed	SinMod
D30	0.152 $\pm$ 0.121	0.215 $\pm$ 0.145
D30F20	0.082 $\pm$ 0.072	0.128 $\pm$ 0.112
D30R10T01P0	0.264 $\pm$ 0.149	0.363 $\pm$ 0.199
D30R20T01P0	0.462 $\pm$ 0.239	0.970 $\pm$ 1.129
D30R20T01P0F20	0.209 $\pm$ 0.139	0.344 $\pm$ 0.224
D30R20T01P3	0.419 $\pm$ 0.228	0.911 $\pm$ 1.099
R20F20	0.244 $\pm$ 0.164	0.416 $\pm$ 0.264
R10	0.161 $\pm$ 0.087	0.220 $\pm$ 0.090
R20	0.104 $\pm$ 0.072	0.174 $\pm$ 0.122

For a more detailed description of the 3D extension of our algorithm and a more comprehensive performance evaluation we address the reader to [8].

### 3.3. Tagged MRI

The proposed algorithm is compared with SinMod [11], available in the InTag plugin for OsiriX. SinMod was shown to perform better than the state-of-the-art HARP in [11]. The evaluation was made on synthetic tMRI sequences, generated with the ASSESS software [12]. The synthetic motion is established on the basis of a 2D analytical model taking typical contraction, relaxation, torsion and thickening of the cardiac muscle into account.

The results obtained on nine simulated sequences are summarized in Table 2. These results show that the proposed algorithm systematically returns the estimate with the smallest mean value and variance, which is a proof of precision and reliability.

To better appreciate the difference in performance, it is useful to analyze the local behavior of each algorithm. This is represented on Fig. 5, where the error images obtained on the 4th frame of the two sequences D30F20 and R20F20, implementing a pure contraction/expansion and pure rotation respectively, is displayed. At that instant, the displacement reaches the

maximum average value and the greatest spatial variation in both cases: in the first case (first row on the Fig. 5) the angular velocity decreases linearly, passing from the endocardial to the epicardial contour; in the second (second row on the Fig. 5) the radial contraction is null on the epicardium and maximal on the endocardium. As shown by the previous results, SinMod is outperformed by the proposed algorithm.

For further results on tMRI sequences we address the reader to [2,13].

## 4. Conclusion

We have described a novel algorithm for the analysis of heart motion from medical images. The displacement is estimated from the monogenic phase and is therefore robust to possible variations of the local image energy. A local affine model accounts for the typical contraction, torsion and shear of myocardial fibers. An effective B-spline multiresolution strategy automatically selects the scale returning the most consistent velocity estimate. The multiresolution strategy together with a least-squares estimate of the monogenic orientation make the algorithm robust under image noise. Due to its general formulation, the proposed algorithm is well suited for measuring myocardial motion from images from different modalities. In particular, we have presented an evaluation on simulated 2D and 3D cardiac ultrasound and tagged MRI sequences. The results have shown that the proposed algorithm is a valid alternative to state-of-the-art techniques in the two fields.

The code for the algorithm presented in this paper is freely online available at the url <http://www.creatis.insa-lyon.fr/ustagging/node/13>.

## Disclosure of interest

The authors declare that they have no conflicts of interest concerning this article.

## Acknowledgments

This work was partially supported by US-Tagging grant financed by Agence Nationale de la Recherche (ANR) and by CNRS.

## References

- [1] Felsberg M, Sommer G. "The monogenic signal". IEEE Trans Image Process 2001;49(12):3136–44.
- [2] Alessandrini M, Basarab A, Liebgott H, Bernard O, "Myocardial motion estimation from medical images using the monogenic signal", IEEE Trans Image Process, in press.
- [3] Felsberg M. "Optical flow estimation from monogenic phase". In: Proceedings of the 1st International Conference on Complex motion, ser. IWCM'04. 2004. p. 1–13.
- [4] Unser M, Sage D, Van De Ville D. "Multiresolution monogenic signal analysis using the riesz laplace wavelet transform". IEEE Trans Image Process 2009;18(11):2402–18.
- [5] Sühling M, Arigovindan M, Jansen C, Hunziker P, Unser M. "Myocardial motion analysis from b-mode echocardiograms". IEEE Trans Image Process 2005;14(4):525–36.

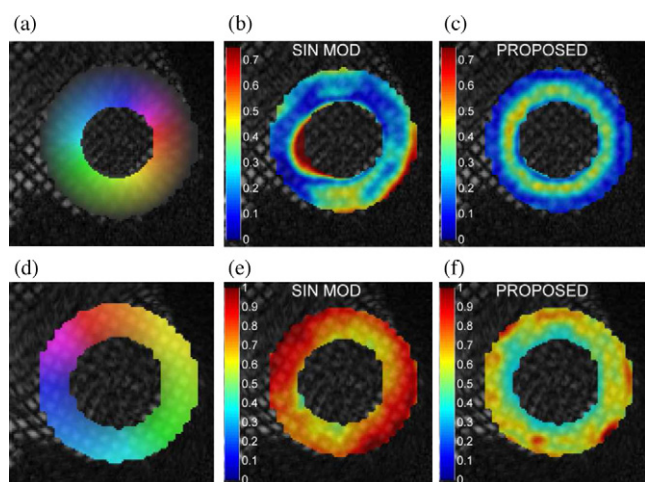


Fig. 5. Error map for the 4th frame of R20F20 (first row) and D30F20 (second row). (a) and (d) denote the benchmark field.

- [6] Alessandrini M, Liebgott H, Friboulet D, Bernard O. “Simulation of realistic echocardiographic sequences for ground truth validation of motion estimation”. In: *Image Processing (ICIP), 2012, 19th IEEE International Conference on*. 2012. p. 2329–32.
- [7] Alessandrini M, Liebgott H, Friboulet D, Bernard O, “Monogenic phase based myocardium motion analysis from cardiac ultrasound with transverse oscillations”, *IEEE International Ultrasonic Symposium (IUS)*, 2012, in press.
- [8] Alessandrini M, Liebgott H, Barbosa D, Bernard O. Monogenic phase based optical flow computation for myocardial motion analysis in 3D echocardiography. *Statistical Atlases and Computational Models of the Heart Imaging Model Challenges 2012*.
- [9] Sermesant M, Chabiniok R, Chinchapatnam P, Mansi T, Billet F, Moireau P, et al. “Patient-specific electromechanical models of the heart for the prediction of pacing acute effects in crt: a preliminary clinical validation”. *Med Image Anal* 2012;16(1):201–15.
- [10] Gao H, Choi HF, Claus P, Boonen S, Jaecques S, van Lenthe G, et al. “A fast convolution-based methodology to simulate 2-d/3-d cardiac ultrasound images”. *IEEE Trans Ultrason Ferroelectr Freq Control* 2009;56(2):404–9.
- [11] Arts T, Prinzen F, Delhaas T, Milles J, Rossi A, Clarysse P. “Mapping displacement and deformation of the heart with local sine-wave modeling”. *IEEE Trans Med Imaging* 2010;29(5):1114–23.
- [12] Clarysse P, Tafazzoli J, Delachartre P, Croisille P. “Simulation based evaluation of cardiac motion estimation methods in tagged-mr image sequences”. *J Cardiovasc Magn Reson* 2011;13:360.
- [13] Alessandrini M, Liebgott H, Basarab A, Clarysse P, Bernard O. “Monogenic signal for cardiac motion analysis from tagged magnetic resonance image sequences”. *Comput Cardiol* 2012:685–8.